Organic Electronics 13 (2012) 1060–1067

Contents lists available at SciVerse ScienceDirect

Organic Electronics

journal homepage: www.elsevier.com/locate/orgel

Electronic structures and chemical reactions at the interface between Li and regioregular poly (3-hexylthiophene)

Xuefei Feng, Wei Zhao [1], Huanxin Ju, Liang Zhang, Yifan Ye, Wenhua Zhang, Junfa Zhu *

National Synchrotron Radiation Laboratory, University of Science and Technology of China, Hefei, Anhui 230029, PR China

ARTICLE INFO

Article history:
Received 10 August 2011
Received in revised form 29 January 2012
Accepted 11 February 2012
Available online 28 February 2012

Keywords:
Metal/π-conjugated polymer interface
Energy level alignment
Synchrotron radiation photoemission spectroscopy
X-ray photoelectron spectroscopy
rr-P3HT
Lithium

ABSTRACT

Interfaces between metals and π-conjugated polymers play an important role in the organic electronic and optoelectronic devices such as polymer-based light-emitting diodes (PLEDs) and photovoltaic devices. In this study, synchrotron radiation photoemission spectroscopy (SRPES) and X-ray photoelectron spectroscopy (XPS) have been applied to in situ investigate the chemical reactions and electronic structure during the interface formation of Li on the regioregular poly(3-hexylthiophene) (rr-P3HT) thin films. Upon Li adsorption onto P3HT at 300 K, Li dopes electrons into P3HT, inducing the occurrence of the P3HT band bending. Moreover, Li can diffuse into the subsurface and react with both S and C atoms in the thiophene rings, leading to the formation of Li_2S and Li–C complex. Compared to the interface of Ca/P3HT, the diffusion/reaction depth of Li is much larger at the Li/P3HT interface. Through the investigation of the evolution of core level and valence band spectra together with secondary electron cutoff an energy level alignment diagram at the Li/rr-P3HT interface is derived.

1. Introduction

In recent years, π-conjugated polymers have attracted significant attentions due to their great potential in the application of polymer-based solar cells (PSCs) [1], light-emitting diodes (PLEDs) [2] and field effect transistors (FETs) [3,4]. Among these polymer-based electronic and optoelectronic devices, one of the common structures is the interface between metal electrodes and semiconducting, π-conjugated polymers. Many studies have demonstrated that these interfaces play an important role in the performance of the devices [5–8]. For instance, the strong chemical reactions between metal electrodes and polymers can destroy the molecular structures of the polymers, which are detrimental to the device performances [9,10]. The electron doping from metals to polymers at the interfaces may result in the appearance of gap states, which would reduce the combination of electrons and holes, and thus influence the performances of PLED devices [5,11–14]. In addition, the interfacial stability and the dynamics have also been found to strongly affect the device performances [15,16]. By comparing the dynamic of interface formation of metals (Ca and Ba) with $OC_1C_{10}PPV$, Janssen et al. found that the diffusion of metals into the polymer resulted in less electron injection and more electron trapping, and consequently, the efficiency and the light output of PLEDs were depressed [15,16].

Thanks to the good conductivity and high electron and hole mobility, the regioregular poly(3-hexylthiophene) (rr-P3HT) and its derivatives have been widely used in polymer light-emitting diodes and polymer solar cells [17–19]. The interfaces between metals and P3HT have been reported for Na, Ca, Cu, Ag, Au, Ti, V and Cr [9,20–23]. It was found that Na, Ca and Cu reacted preferentially with S atoms of P3HT, leading to the formation of metal sulfides, while Ti, V, Cr reacted with both S and C atoms of the P3HT. However, no obvious chemical interaction at

* Corresponding author. Tel.: +86 551 3602064.
E-mail address: jfzhu@ustc.edu.cn (J.F. Zhu).
[1] Present address: Lehrstuhl für Physikalische Chemie II, Universität Erlangen-Nürnberg, Egerlandstraße 3, 91058 Erlangen, Germany.

1566-1199/$ - see front matter © 2012 Elsevier B.V. All rights reserved.
http://dx.doi.org/10.1016/j.orgel.2012.02.007

the interfaces between Ag, Au and P3HT was found. Moreover, for the Ca/P3HT interface, Ca was found to diffuse 3 nm into the polymer subsurface to react with S, leading to the formation of $(CaS)_n$ clusters [21]. Upon Ca deposition, the HOMO of P3HT was strongly affected and a downward band bending which facilitate the injection of electrons was found. However, no polaron or bipolaron was found near the Fermi level [9]. Although Li is also a low work function metal (Φ = 2.9 eV) [24] and often used as the electrode of PLEDs [6], to our knowledge, no prior study on Li/P3HT interface can be found.

In this study, synchrotron radiation photoemission spectroscopy (SRPES) and X-ray photoelectron spectroscopy (XPS) were employed to in situ investigate the interface formation between Li and P3HT. In contrast to Ca on P3HT where Ca exclusively reacts with S atoms was found [21], the chemical reactions of Li with both S and C atoms of P3HT were observed. In addition, the changes of valance bands with Li coverages and the energy level alignment diagram at the Li/P3HT interface have been derived. Finally, the interfacial reactions and diffusion of Li on P3HT are discussed.

2. Experimental

The regioregular poly(3-hexylthiophene), whose molecular structure is shown in Fig. 1, with MW ≈ 30,000 amu was obtained from Howe Electronic Colorant Ltd., Hong Kong. The thin P3HT film was prepared by spin-coating the P3HT/chloroform solution (5 mg/ml) directly onto the clean gold-coated silicon wafer with 1000 rpm for 10 s, followed by 2000 rpm for 60 s in dry nitrogen atmosphere. We introduced 100 nm gold on the clean silicon wafer in order to increase the conductivity of the substrate. It was done on each sample for four times with 60 μl of the solution dropped in each step. The thickness of the polymer film is about 100 nm ensured by atomic force microscopy (AFM), as described in Ref. [19]. After preparation, the sample was placed into ultrahigh vacuum (UHV) immediately to avoid photodegradation or oxidation. Before Li deposition, the sample was annealed to 120 °C (below the glass transition temperature (T_g) of 214 °C which was reported by product company) for 30 min, in order to remove any residual solvent and surface contaminant. After these treatments, no Cl or O signal can be detected by XPS, and the ratio of C and S atoms is about 10:1, in excellent agreement with the stoichiometric ratio of C and S in P3HT.

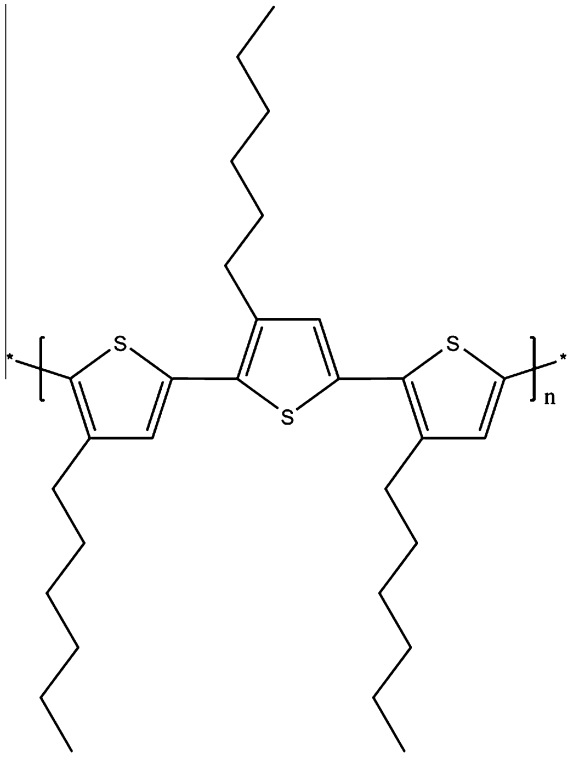

Fig. 1. Molecular structure of regioregular poly(3-hexylthiophene).

The experiments were carried out in two separate UHV systems. The SRPES measurements were performed in Surface Physics Endstation at beamline U18 in the National Synchrotron Radiation Laboratory (NSRL) in Hefei, China. The detailed description can be found elsewhere [9]. Briefly, the endstation is connected to a bending magnet and equipped with three gratings. It covers the range of the photon energy from 10 to 250 eV, and the resolving power ($E/\Delta E$) is better than 1000. This endstation contains three UHV chambers: analysis chamber, sample preparation chamber and molecular beam epitaxy (MBE) chamber. The base pressures are 4×10^{-11}, 1×10^{-10} and 2×10^{-10} mbar, respectively. The analysis chamber is equipped with a VG ARUPS10 angle-resolved photoelectron spectrometer, a twin anode X-ray source, an Ar^+ sputter gun and a retractable four-grid optics for low energy electron diffraction (LEED). The sample preparation chamber houses a small hemispherical electron energy analyzer, a cold cathode ion source, an electron gun and connects with a sample load–lock system. The MBE chamber comprises an electron gun for reflection high energy electron diffraction (HREED), a quartz crystal microbalance (QCM) for measuring the deposition rates and several Knudsen cell evaporators. The deposition rate of Li was about 0.77 Å/min, as measured by monitoring the attenuation of Au 4f XPS signal after Li deposition on an Au-coated silicon wafer. Note that the thickness reported in this paper is defined by the Li dose (i.e., the deposition rate multiply time), which is so called "nominal thickness". As the sticking probability of Li on P3HT is expected to be less than 1, the amount of Li adsorbs on P3HT is thus less than the Li dose during the deposition.

The XPS measurements were performed on a VG MARK II spectrometer, which has been described in detail previously [25]. Briefly, this spectrometer comprises three UHV chambers: analysis chamber, preparation chamber and scanning tunneling microscope (STM) chamber. The analysis chamber with the base pressure of 6×10^{-11} mbar is equipped with a hemispherical electron analyzer, a twin-anode X-ray gun, a He discharge lamp for ultraviolet photoemission spectroscopy (UPS), an electron gun and a quadrupole mass spectrometer instrument (Pfeiffer QMG 220). The preparation chamber connects with a sample

load–lock system and comprises a LEED optics, a cold cathode ion gun for sample cleaning and several evaporators, and the base pressure is 1×10^{-10} mbar. The chamber for STM experiments has a base pressure is 1×10^{-10} mbar and houses an Arrhus STM probe, an Ar^+ sputter gun and a multiple sample holder for sample storage and treatment.

For XPS experiments, Mg Kα source ($h\upsilon$ = 1253.6 eV) was chosen and the overall energy resolution was 0.9 eV [25]. The spectra were taken at normal emission and all reported binding energies were referenced to the Au 4f binding energy of a clean Au(111) single crystal. The work function measurements were conducted with a bias voltage of −6 V introduced to the sample in order to allow the observation of the secondary electron cut-off.

3. Results

3.1. Synchrotron radiation photoemission spectroscopy (SRPES)

Fig. 2a shows the S 2p SRPES spectra as a function of the thickness of Li. These spectra were measured with photon energy of 200 eV and an emission angle of 0° with respect to the surface normal. On the clean P3HT surface, two peaks locate at 166.2 and 165.0 eV, which are assigned to S $2p_{1/2}$ and $2p_{3/2}$, respectively. We label these original two peaks as "unreacted" S. Upon Li deposition, the following changes can be observed immediately: (1) the damping of the "unreacted" S 2p peaks; (2) the appearance of two new S 2p peaks at about 3.1 eV lower binding energy relative to the original S 2p signal (163.1 eV and 161.9 eV, respectively); and (3) the shifts of both the original and new S 2p signals towards higher binding energies. According to previous investigations of Ca, Na, Cu, Ag, Ti, V and Cr on P3HT [9,20,22,23], these two new peaks can be ascribed to the reaction between Li and S atoms, leading to the formation of Li_2S. This indicates that Li reacts strongly with S atoms in the thiophene rings. For clarity, we label them as "reacted" S. The 3.1 eV shift toward lower binding energy relative to the "unreacted" S 2p is slightly larger than the 2.8 eV shift observed at the Ca/P3HT interface [21]. After about 3 Å Li is deposited, the "reacted" S 2p signal reaches its maximum intensity at the expense of the "unreacted" S 2p signal. The shifts of both the "reacted" and "unreacted" S 2p peaks toward higher binding energies with increasing Li thickness are typically due to the downward band bending effect which is associated with the long-range electron donation into the polymer [20,21].

The Li 1s spectra obtained with photon energy of 150 eV as a function of Li thickness are displayed in Fig. 2b. After 0.13 Å Li is deposited, a peak at 56.4 eV appears. With increasing Li dose, this peak grows with intensity and almost unchanged binding energy. With respect to the Li 1s spectrum from a bulk-like Li film (not shown), the spectra shown here shift by 1.4 eV toward higher binding energies, indicating that in the range of the thickness studied in this experiment all metallic Li atoms become Li^+ ions after they adsorb on P3HT. This further proves that a strong reaction occurs between Li and P3HT.

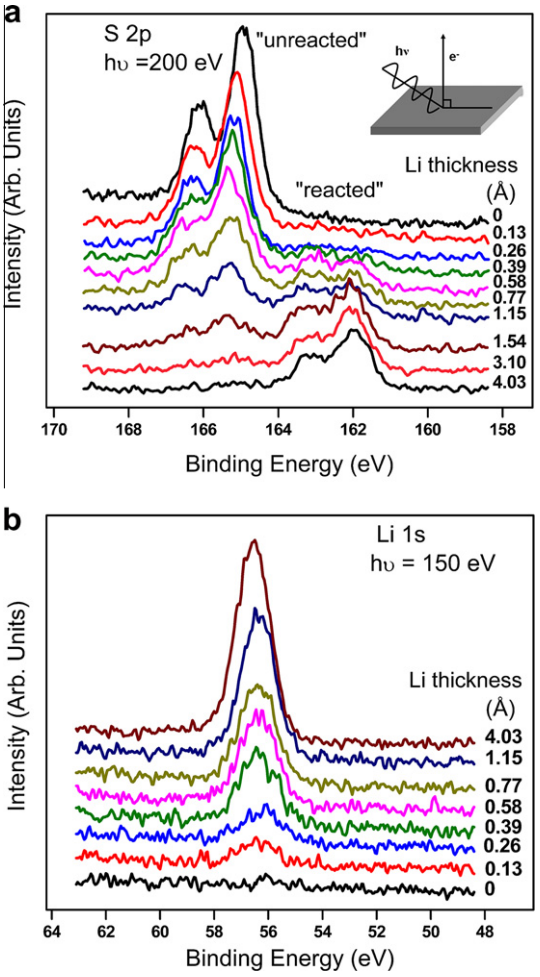

Fig. 2. SRPES spectra of (a) S 2p and (b) Li 1s region for Li deposition on rr-P3HT measured with photon energies of 200 and 150 eV, respectively. The insert in (a) shows the geometry of the experiment. The measurements were performed in a stepwise manner.

3.2. X- ray photoelectron spectroscopy (XPS)

Since metal atoms could diffuse into the subsurface of polymers after they were deposited [15,16], in order to gain the information from different depth, we did similar experiments using a different excitation photon energy. As compared to using 200 eV photons as the excitation source for S 2p, it is obvious that the probe depth is much deeper when we use the Mg Kα radiation ($h\upsilon$ = 1253.6 eV) as the excitation source. Fig. 3a shows the S 2p XP spectra using Mg Kα radiation from the P3HT surface deposited with different Li thicknesses. Same as the observation excited with 200 eV photons (Fig. 2a), the binding energy of S 2p also shifts toward higher binding energies with increasing Li thickness due to the band bending effect. Moreover, the binding energy difference of "reacted" and "unreacted" S 2p is also 3.1 eV, indicating that the reaction between Li and S atoms is uniform within the whole probe depth. However, in contrast to Fig. 2a, here the new S 2p peaks (marked with "reacted") can be only clearly

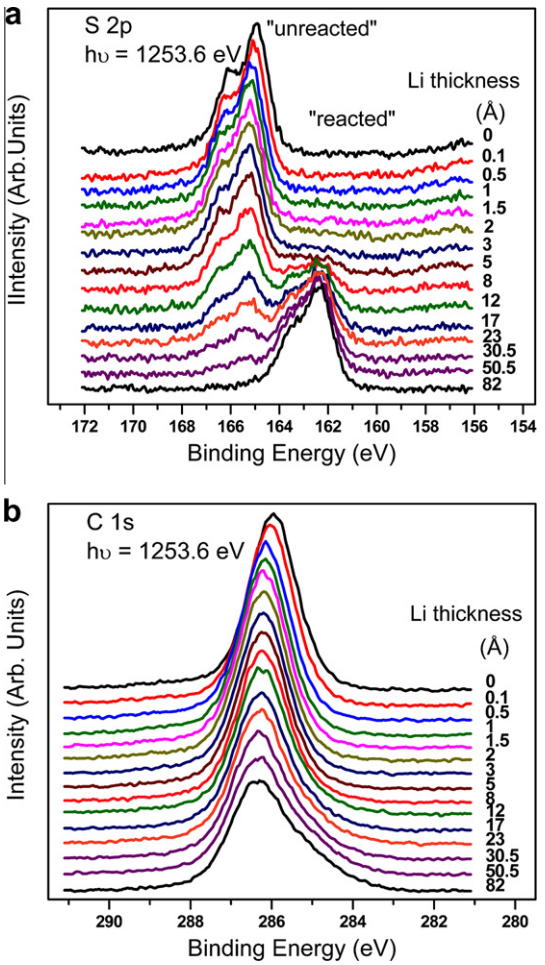

Fig. 3. XP spectra of S 2p (a) and C 1s (b) from the P3HT surface with different Li thicknesses. The excitation photon energy is 1253.6 eV. The binding energy difference between "unreacted" and "reacted" S 2p signals is about 3.1 eV.

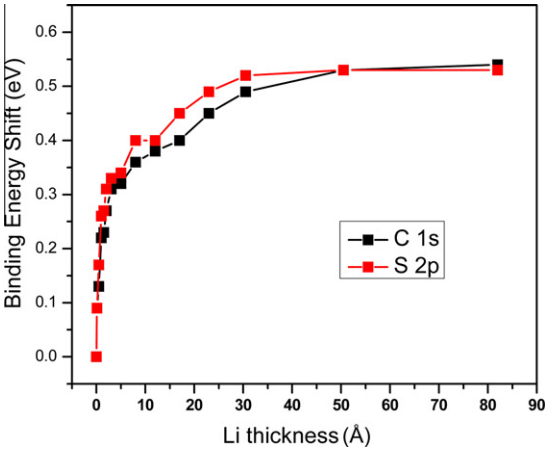

Fig. 4. Binding energy shifts as a function of Li dose for S 2p and C 1s. The data are taken from Fig. 3a and b, respectively.

observed after 3 Å Li is deposited. We attribute this to the increased probe depth, similar to previous observation for Ca on P3HT [21]. Consequently, the original "unreacted" S 2p signal is still visible even at the Li thickness of 30 Å. Compared to the Ca/P3HT system [21], the attenuation of the S 2p signal is much weaker at the same amount of Li deposited onto P3HT. This may arise from two possible reasons: (1) The sticking probability of Li on P3HT is lower than Ca, resulting in lower coverage on P3HT at the same dose; (2) The diffusion effect of Li at the interface is much stronger than Ca.

Fig. 3b presents the C 1s XP spectra for various Li thicknesses on P3HT. The spectra were also recorded with the Mg Kα radiation. Upon Li deposition, besides the binding energy of C 1s peak shifts toward higher binding energies, the C 1s spectra get broader and become asymmetric at high Li doses. Fig. 4 plots the binding energy shifts for both S 2p and C 1s as a function of Li dose. The almost identical binding energy shifts for both core-levels further confirm that there is a downward band bending of P3HT after Li deposition. Since the maximum binding energy shift toward high binding energies is about 0.52 eV, the bands must bend downward by 0.52 eV to facilitate the electron injection.

In contrast to the interfaces of P3HT with Na and Ca [9,20,21] where only reactions between metals and S atoms were observed, in the present case, except for the reaction between Li and S atoms, the change of C 1s spectra during the interface formation of Li/P3HT implies that Li may also react with C atoms of P3HT. More discussions can be seen in Section 4.1.

3.3. Valence band spectra

Fig. 5 displays secondary cutoff and valance band spectra at the photon energy of 26 eV as a function of Li thickness on P3HT. In the valance band region, the peak at about

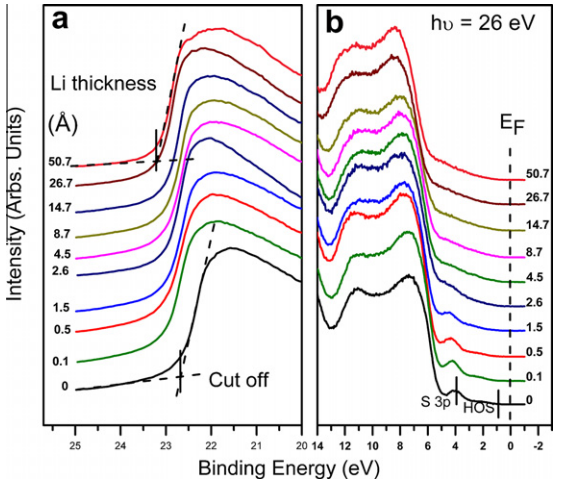

Fig. 5. The evolution of secondary cutoff (a) and valance band (b) spectra with increasing Li thickness. The photon energy is 26 eV. The secondary cutoff region was normalized in order to enable easy and direct comparison.

3.95 eV from the clean P3HT surface is assigned to the contribution of the pure π-character S 3p [10,26]. From Fig. 5b, we can derive that the highest-occupied molecular orbital (HOMO) is at about 1.5 eV and the HOMO cutoff (i.e., the highest occupied states (HOS)) locates at 0.92 eV, in agreement with previous results [9,20]. The ionization potential (IP) of P3HT determined from the width of the valence band spectrum is 4.27 eV, in close agreement with those reported by Zhao et al. [9] (4.25 eV) and Schmeisser [27] (4.2 eV), but slightly larger than that reported by Mikalo and Schmeisser (4.13 eV) [20]. The level of the lowest unoccupied states (LUS) of P3HT can be determined if the energy band gap (E_g) of P3HT is known. Since the E_g of bulk P3HT or bulk-like P3HT film is not available in the literature, here we use the optical band gap ($E_{g,opt}$) of P3HT (2.3 eV [28]) instead by ignoring the exciton binding energy to determine the LUS position of P3HT, similar as previous studies of Na/P3HT [20] and Ca/P3HT [9]. This yields the LUS of P3HT located at 1.38 eV above the Fermi level. It should be mentioned that $E_{g,opt}$ is usually 0.3–0.4 eV smaller than E_g [29]. Although E_g of ultrathin P3HT film has been reported by Kanai et al., it is found that this E_g varies with the substrate on which P3HT was spin-coated and the annealing temperature [30], and, thus, is expected to be different from the value of bulk-like P3HT film. In fact, Liao et al. found that it is even more appropriate to determine the LUS position by using $E_{g,opt}$ [31].

After Li is deposited on P3HT, both S 3p and HOS shift toward higher binding energies, which can be ascribed to the band bending effect. Moreover, the HOMO of P3HT broadens with increasing Li thickness. In contrast to the interfaces of alkali metals/PFO and Ca/PPV where new density of states (DOS) between Fermi level and HOS (i.e., so-called gap states) have been observed [5,32], here no gap states can be observed although the π levels of the polymer are strongly affected, similar to the results found in the case of Na/P3HT [28]. As shown in Fig. 5a, the secondary cutoff shifts continuously toward higher binding energies upon Li deposition onto P3HT, indicating the decrease of work function. After 50 Å Li is deposited, the shift of the secondary cutoff reaches the maximum value of 0.55 eV, suggesting that the work function decreases by 0.55 eV. However, the HOS position cannot be clearly identified at this coverage. Since the band bending affects the binding energy of each band identically, the shifts of the HOS and LUS bands can be deduced from the shifts of C 1s and S 2p. After the P3HT surface is deposited with 50 Å Li, from Fig. 4 one can see that both C 1s and S 2p shift +0.52 eV. This is indicative of a downward band bending of 0.52 eV. Therefore, both HOS and LUS should bend downwards by 0.52 eV. The interface dipole, as determined from the sum of the band bending and shift of secondary cutoff, is 0.03 eV, suggesting that there is only weak interface dipole existing after 50 Å Li is deposited.

From the analysis above, we can schematically plot the energy band alignment diagram at the interface between Li and P3HT, which is shown in Fig. 6. The right side of Fig. 6 shows the bands for a bulk-like Li film, which was obtained by depositing a thick (>400 Å) Li films on top of P3HT. From this thick Li film, the work function can be determined to be 2.91 eV, which matches very well with the value

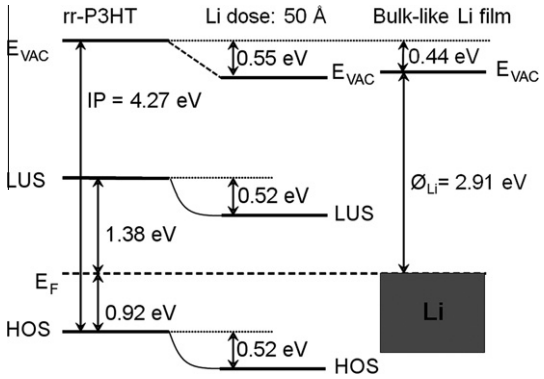

Fig. 6. Schematic drawing of the energy level alignment diagram at the Li/P3HT interface.

2.90 eV reported previously for bulk metallic Li [24]. As seen in Fig. 6, the barrier for electron injection decreases by 0.52 eV after 50 Å Li is deposited on P3HT.

4. Discussion

4.1. Interfacial reaction

As mentioned above, the appearance of new S 2p species after P3HT is deposited with Li, as shown in Figs. 2a and 3a, clearly suggests that there is a strong chemical reaction between Li and S atoms, similar to the observations in the case of Ca, Na, Cu, Ag, Ti, V and Cr on P3HT [9,20,22,23]. However, in contrast to the interfaces of Ca, Na, Cu and Ag on P3HT where the interface reactions were only observed between metal and S atoms, in the present case C 1s gradually broadens and a new shoulder is distinguishable at lower binding energy side after Li is deposited on P3HT. To gain further information, we have deconvoluted the C 1s spectra from P3HT before and after Li deposition. Fig. 7 shows the C 1s spectra and their deconvolution from pristine P3HT and the surface covered by 50 Å Li. As seen in the chemical structure of P3HT shown in Fig. 1, each pristine P3HT repeat unit contains 6 saturated aliphatic carbon atoms in the side chain and 4 unsaturated aromatic carbon atoms in the thiophene ring. Assuming that these two different C groups have different binding energies, the C 1s spectrum from clean P3HT, therefore, can be deconvoluted into two components with an intensity ratio of 3:2: the saturated and unsaturated carbon atoms [33,34]. As shown in Fig. 7a, using the binding energy difference of 0.4 eV and equal widths [33,34], we fitted the clean P3HT C 1s spectrum with two components whose peak positions locate at 285.8 eV and 286.2 eV, attributed to saturated and unsaturated carbon, respectively. The resulting intensity ratio of the two components is about 3:2, in good agreement with the chemical structure of P3HT. After 50 Å Li is deposited on P3HT, a shoulder emerging at the lower binding energy side can be seen clearly (see Fig. 7b). In order to determine the position of new C 1s peak, we took the difference C 1s spectrum with respect to clean P3HT through the following procedure: (i) First, the C 1s spectrum was shifted 0.52 eV towards lower binding energy to eliminate the

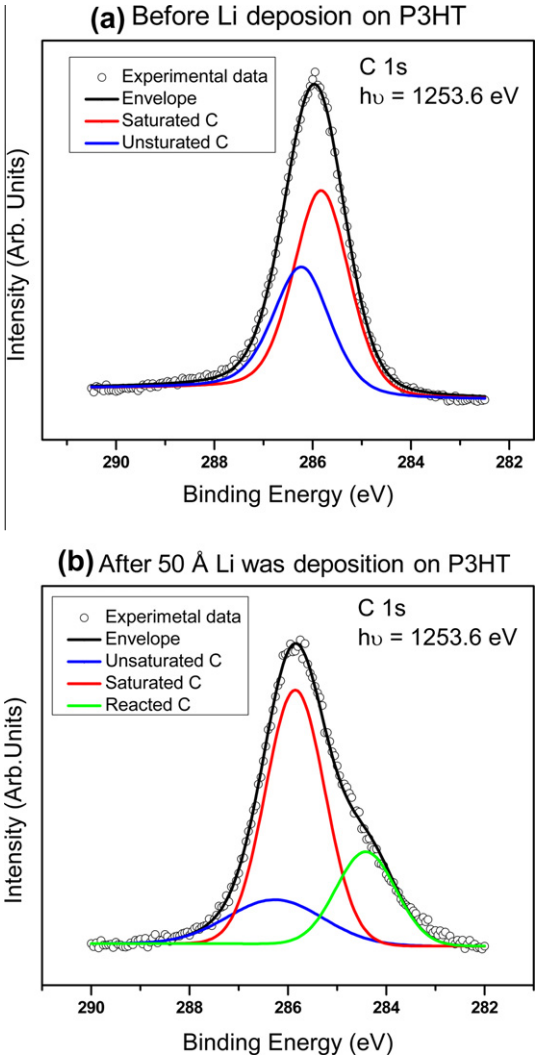

Fig. 7. XP spectra of C 1s region (a) before and (b) after 50 Å Li was deposited onto the P3HT surface. The black open circles are the experimental data. The red and blue lines present the saturated and unsaturated C, respectively. The green line in (b) shows the signal of the new C 1s peak. The black lines indicate the sum of individual components. (For interpretation of the references to colour in this figure legend, the reader is referred to the web version of this article.)

band bending effect; (ii) Then we normalized the intensity of C 1s main peak to that of clean P3HT to eliminate the damping effect. From the difference spectrum, a new peak with a binding energy of 1.4 eV lower than that of the saturated carbon (thereafter we call it as "reacted" C) can be distinguished. Taking this new C 1s species into account, we fitted the C 1s spectrum from 50 Å Li covered P3HT with three components and the results are shown in Fig. 7b. As seen, almost no change in the intensity of the saturated carbon can be observed, implying that the aliphatic carbon atoms are very stable and not affected by Li deposition. However, the intensity of unsaturated carbon atoms has a large decrease; the intensity ratio between saturated aliphatic carbon and unsaturated carbon is about 3:1. While the intensity ratio of saturated carbon and the sum of unsaturated carbon and "reacted" C still keeps 3:2, implying that the "reacted" C originates from the conversion of unsaturated carbon. This result indicates that after 50 Å Li is deposited on P3HT, not only S atoms but also C atoms in the thiophene rings can react with Li.

The above reaction mechanism between Li and C atoms of P3HT is different from what was reported previously for the interfacial reactions between Ti, V, Cr and P3HT where the reaction between metal and C atoms also took place [23]. Instead of giving specific C atoms for reaction, they claimed the reactions of these transition metals with P3HT involving the d orbitals of the metals, leading to an unpaired metal d electron and resultant p–d spin–spin broadening of the metal 2p peaks [23,35,36]. However, Li ($1s^2 2s^1$) contains no d orbitals, it is understandable that the reaction mechanism with P3HT is different from those metals. Similar to Li, aluminum also contains no d orbitals; the study of chemical reactions of Al with similar molecules to P3HT, i.e., α-sexithiophene (6T) and poly-3-otylthiophene (P3OT), showed that Al reacts with α–C in the thiophene rings to form Al–C bonds [10]. Since the α–C atoms in P3HT belong to the group of unsaturated C, the decrease of the intensity after Li deposition suggests that the interaction of Li with the α–C atoms is thus possible.

However, in comparison with Ca/P3HT where only reactions between Ca and S atoms were observed [21,34], the reaction at the interface of Li and P3HT seems to be stronger since Li can react with both S and C atoms. This may be related to the smaller electronegativity of Li (0.98) than Ca (1.0) [37] and the smaller atomic size of Li than Ca. One may notice that the electronegativity of Na (0.8) is even smaller than that of Li, however, at the interface of Na/P3HT only the reaction between Na and S atoms was reported by Mikalo and Schmeisser [20]. No obvious evidence for the reaction of Na with C atoms up to the maximum Na exposure they studied was found. However, at the similar exposure as they used, we also could not observe the obvious C 1s shoulder at the low binding energy side. Only at higher exposures, the reaction of Li with C atoms can be gradually observed. Therefore, for the Na/P3HT case, it would be interesting to measure the evolution of C 1s spectra at higher Na exposures. To truly understand the differences in the reaction mechanisms of P3HT with these metals, further theoretical calculations are definitely needed.

It is worth to mention that we have excluded the possibility of the new C 1s peak at the low binding energy side after Li deposition originating from the background contamination such as CO and CO_2 adsorption. To prove this, a controlled experiment with same experimental environments has been done by depositing a thick Li film on an Au-coated Si wafer and leaving it in the UHV chamber for a long period. Since the fresh metallic Li film is very reactive, it should easily react with residual gas such as CO or CO_2 in the vacuum. However, after about 16 h in UHV, the C 1s XPS spectrum only shows a very small C 1s peak at about 286.5 eV, which is 0.8 eV higher than the binding energy of "reacted" C (spectrum not shown) and this binding energy difference should be even larger if the band bending effect occurred on Li/P3HT is not considered.

Therefore, the "reacted" C cannot be related to any background contamination of C-containing species.

4.2. Diffusion and reaction depth

From the S 2p and C 1s spectra shown in Fig. 3a and b, the changes in intensity of S 2p and C 1s as a function of Li thickness are displayed in Fig. 8. As can be seen, upon Li deposition, the total intensities of both S 2p and C 1s decrease immediately with the rate that the former is faster than the later. This can be interpreted with the following model: since the outmost surface of P3HT is terminated by the side alkyl chains and the conjugate backbones (the thiophene rings) are shielded by these "saturated C" [30,38], upon Li deposition, Li diffuses into the subsurface to react with the S and/or C atoms in the thiophene rings. This leads to the damping of both S and C signals. However, since topmost C atoms from side alkyl chains do not react with Li and they are not damped by Li deposition at low coverages, the intensity of C 1s signal decreases slower than that of S 2p. Similar phenomenon can also been found at the Ca/P3HT interface up to 10 ML Ca deposited on P3HT [21]. In comparison with Ca/P3HT where the S 2p spectra showed that before the original "unreacted" S signal completely disappears, both "reacted" and "unreacted" S signals start to decrease in intensity because of the formation of continuous metallic Ca film on top of the surface. Here the increase of "reacted" S intensity does not reach its maximum until all the S atoms react with Li within the XPS probing depth. Therefore, the depth of the reaction and diffusion at the Li/P3HT interface is much deeper than that at the Ca/P3HT interface. Since the mean free path (λ) of S 2p photoelectrons at present measured photon energy of 1253.6 eV is about 41 Å [39], the "unreacted S" cannot be detected after 82 Å Li deposition, indicates that the reaction depth at the Li/P3HT interface is at least 120 Å (3λ), much larger than the reaction depth of 3 nm at the Ca/P3HT interface [21]. It should be noted that this reaction/diffusion depth is estimated based on the assumption that Li atoms do not form three-dimensional clusters on the surface up to 82 Å and homogeneously distribute in/on P3HT. In fact, the Li 1s XPS spectra (not shown) demonstrate that only ionic Li species, like shown in Fig. 2b, can be observed up to 82 Å, suggesting that the deposited Li atoms do not form metallic clusters on the P3HT surface and they most likely diffuse into subsurface to react with S and C atoms of P3HT.

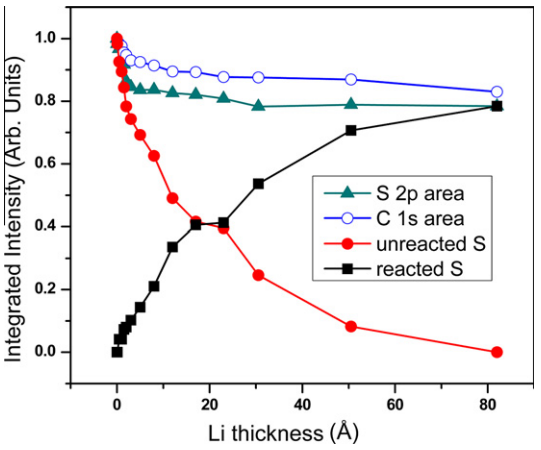

Fig. 8. Integrated intensities of the S 2p and C 1s signals from the spectra shown in Fig. 3 (normalized to those from the clean P3HT surface) as a function of Li thickness. For S 2p, the intensities of the components from reacted and unreacted S are additionally displayed, respectively.

Note that although the low barrier for electron injections at the interface of P3HT with Li facilitates the electron injection, the strong chemical reactions between Li and P3HT can destroy the π-conjugate structures of P3HT. Therefore, when Li is used as the electrode in the P3HT-based electronic and optoelectronic devices such as PLEDs, a thin buffer layer should be inserted into the interface between Li and P3HT to protect P3HT from degradation and prevent the strong Li diffusion.

5. Conclusions

In this work, SRPES and XPS have been applied to study the interface between Li and rr-P3HT. The results indicate that the charges transfer from Li to P3HT occurs, leading to a downward band bending. In addition, besides the reaction between Li and S atoms which leads to the formation of the lithium sulfide, at high Li thickness, the reaction of Li with C atoms in thiophene rings of P3HT is also found, which is different from the interfaces between Ca, Na, Al, Cu, Ag, Au, Ti, V, Cr and P3HT. The valence band spectra show that after 50 Å Li is deposited on P3HT, the work function is reduced by 0.55 eV. No polaron or bipolaron states can be found near the Fermi edge. From the SRPES and XPS data, a clear energy level alignment diagram at the Li/P3HT interface has been derived. Moreover, a deeper diffusion and reaction depth at the Li/P3HT interface is observed as compared to the Ca/P3HT interface.

Acknowledgements

We gratefully acknowledge the National Natural Science Foundation of China (Grant No. 20773111, 21173200), the Specialized Research Fund for the Doctoral Program of Higher Education (SRFDP) of Ministry of Education (Grant No. 20113402110029), the "Hundred Talents Program" of the Chinese Academy of Sciences, and National Basic Research Program of China (2010CB923302) for the financial support of this work. W.Z acknowledges the National Natural Science Foundation of China (Grant No. 11175172).

References

[1] Y. Kim, S. Cook, S.M. Tuladhar, S.A. Choulis, J. Nelson, J.R. Durrant, D.D.C. Bradley, M. Giles, I. McCulloch, C.S. Ha, M. Ree, Nat. Mater. 5 (2006) 197.
[2] H. Fei, Z. Yong, M.S. Liu, A.K.Y. Jen, Adv. Funct. Mater. (2009) 2457.
[3] H. Sirringhaus, N. Tessler, R.H. Friend, Science 280 (1998) 1741.
[4] N. Stutzmann, R.H. Friend, H. Sirringhaus, Science 299 (2003) 1881.
[5] M.K. Fung, S.L. Lai, S.N. Bao, C.S. Lee, S.T. Lee, W.W. Wu, M. Inbasekaran, J.J. O'Brien, J. Vac. Sci. Technol. A 20 (2002) 911.
[6] E.I. Haskal, A. Curioni, P.F. Seidler, W. Andreoni, Appl. Phys. Lett. 71 (1997) 1151.

[7] J. Frisch, H. Glowatzki, S. Janietz, N. Koch, Org. Electron. 10 (2009) 1459.
[8] Y.H. Zhou, L.P. Zhu, Y. Qiu, Org. Electron. 12 (2011) 234.
[9] W. Zhao, Y.X. Guo, X.F. Feng, L. Zhang, W.H. Zhang, J.F. Zhu, Chin. Sci. Bull. 54 (2009) 1978.
[10] P. Dannetun, M. Boman, S. Stafstrom, W.R. Salaneck, R. Lazzaroni, C. Fredriksson, J.L. Bredas, R. Zamboni, C. Taliani, J. Chem. Phys. 99 (1993) 664.
[11] L.S. Liao, M.K. Fung, L.F. Cheng, C.S. Lee, S.T. Lee, M. Inbasekaran, E.P. Woo, W.W. Wu, Appl. Phys. Lett. 77 (2000) 3191.
[12] L.S. Liao, L.F. Cheng, M.K. Fung, C.S. Lee, S.T. Lee, M. Inbasekaran, E.P. Woo, W.W. Wu, Phys. Rev. B 62 (2000) 10004.
[13] G. Greczynski, M. Fahlman, W.R. Salaneck, J. Chem. Phys. 113 (2000) 2407.
[14] G. Greczynski, M. Fahlman, W.R. Salaneck, Appl. Surf. Sci. 166 (2000) 380.
[15] F.J.J. Janssen, A.W.D. van der Gon, L.J. van Ijzendoorn, R. Thoelen, M.J.A. de Voigt, H.H. Brongersma, Appl. Surf. Sci. 241 (2005) 335.
[16] F.J.J. Janssen, L.J. van Ijzendoorn, A.W.D. van der Gon, M.J.A. de Voigt, H.H. Brongersma, Phys. Rev. B 70 (2004) 165425.
[17] Z.Y. Liu, D.W. He, Y.S. Wang, H.P. Wu, J.G. Wang, Synth. Met. 160 (2010) 1036.
[18] L. Motiei, Y. Yao, J. Choudhury, H. Yan, T.J. Marks, M.E. van der Boom, A. Facchetti, J. Am. Chem. Soc. 132 (2010) 12528.
[19] J.S. Kim, Y. Lee, J.H. Lee, J.H. Park, J.K. Kim, K. Cho, Adv. Mater. 22 (2010) 1355.
[20] R.P. Mikalo, D. Schmeisser, Synth. Met. 127 (2002) 273.
[21] J.F. Zhu, F. Bebensee, W. Hieringer, W. Zhao, J.H. Baricuatro, J.A. Farmer, Y. Bai, H.P. Steinruck, J.M. Gottfried, C.T. Campbell, J. Am. Chem. Soc. 131 (2009) 13498.
[22] A. Lachkar, A. Selmani, E. Sacher, M. Leclerc, R. Mokhliss, Synth. Met. 66 (1994) 209.
[23] A. Lachkar, A. Selmani, E. Sacher, Synth. Met. 72 (1995) 73.
[24] H.B. Michaelson, J. Appl. Phys. 48 (1977) 4729.
[25] M. Chen, X.F. Feng, L. Zhang, H.X. Ju, Q. Xu, J.F. Zhu, J.M. Gottfried, K. Ibrahim, H.J. Qian, J.O. Wang, J. Phys. Chem. C 114 (2010) 9908.
[26] W.R. Salaneck, O. Inganas, B. Themans, J.O. Nilsson, B. Sjogren, J.E. Osterholm, J.L. Bredas, S. Svensson, J. Chem. Phys. 89 (1988) 4613.
[27] D. Schmeisser, Synth. Met. 138 (2003) 135.
[28] R.K. Meyer, R.E. Benner, Z.V. Vardeny, M. Liess, M. Ozaki, K. Yoshino, Y. Ding, T. Barton, Synth. Met. 84 (1997) 549.
[29] S.F. Alvarado, P.F. Seidler, D.G. Lidzey, D.D.C. Bradley, Phys. Rev. Lett. 81 (1998) 1082.
[30] K. Kanai, T. Miyazaki, H. Suzuki, M. Inaba, Y. Ouchi, K. Seki, Phys. Chem. Chem. Phys. 12 (2010) 273.
[31] L.S. Liao, M.K. Fung, C.S. Lee, S.T. Lee, M. Inbasekaran, E.P. Woo, W.W. Wu, Appl. Phys. Lett. 76 (2000) 3582.
[32] L. Dong Won, K. Kyungkon, J. Jung-Il, P. Yungsup, Synth. Met. 143 (2004) 181.
[33] E.L. Ratcliff, J.L. Jenkins, K. Nebesny, N.R. Armstrong, Chem. Mater. 20 (2008) 5796.
[34] F. Bebensee, J.F. Zhu, J.H. Baricuatro, J.A. Farmer, Y. Bai, H.P. Steinruck, C.T. Campbell, J.M. Gottfried, Langmuir 26 (2010) 9632.
[35] D.A. Steigerwald, W.F. Egelhoff, Surf. Sci. 192 (1987) L887.
[36] A. Stamant, D.R. Salahub, Chem. Phys. Lett. 169 (1990) 387.
[37] A.L. Allred, J. Inorg. Nucl. Chem. 17 (1961) 215.
[38] X.T. Hao, T. Hosokai, N. Mitsuo, S. Kera, K. Mase, K.K. Okudaira, N. Ueno, Appl. Phy. Lett. 89 (2006) 182113.
[39] B. Lesiak, A. Kosinski, A. Jablonski, L. Kover, J. Toth, D. Varga, I. Cserny, M. Zagorska, I. Kulszewicz-Bajer, G. Gergely, Appl. Surf. Sci. 174 (2001) 70.